

Astroparticle Phys., submitted 11 October 2002  
 revised 19 November 2002

## TeV gamma rays and cosmic rays from the nucleus of M87, a mis-aligned BL Lac object

R.J. Protheroe<sup>1,\*</sup>, A.-C. Donea<sup>1</sup>, A. Reimer<sup>2</sup>

<sup>1</sup>Department of Physics and Mathematical Physics, The University of Adelaide,  
 Adelaide, SA 5005, Australia

<sup>2</sup>Ruhr-Universität Bochum, Institut für Theoretische Physik, Lehrstuhl IV: Weltraum-  
 und Astrophysik, D-44780 Bochum, Germany

### Abstract

The unresolved nuclear region of M87 emits strong non-thermal emission from radio to X-rays. Assuming this emission to originate in the pc scale jet aligned at  $\theta \sim 30^\circ$  to the line of sight, we interpret this emission in the context of the Synchrotron Proton Blazar (SPB) model. We find the observed nuclear jet emission to be consistent with M87 being a mis-aligned BL Lac Object and predict gamma-ray emission extending up to at least 100 GeV at a level easily detectable by GLAST and MAGIC, and possibly by VERITAS depending on whether it is high-frequency or low-frequency peaked. Predicted neutrino emission is below the sensitivity of existing and planned neutrino telescopes. Ultra-high energy neutrons produced in pion photoproduction interactions decay into protons after escaping from the host galaxy. Because energetic protons are deflected by the intergalactic magnetic field, the protons from the decay of neutrons emitted in all directions, including along the jet axis where the Doppler factor and hence emitted neutron energies are higher, can contribute to the observed ultra-high energy cosmic rays. We consider the propagation of these cosmic ray protons to Earth and conclude that M87 could account for the observed flux if the extragalactic magnetic field topology were favourable.

### PACS:

- 98.54.Cm Active and peculiar galaxies (including BL Lacertae objects, blazars, Seyfert galaxies, Markarian galaxies, and active galactic nuclei)
- 98.54.Gr Radio galaxies
- 98.58.Fd Jets, outflows and bipolar flows
- 98.70.Rz gamma-ray sources
- 98.70.Sa Cosmic rays (including sources, origin, acceleration, and interactions)
- 13.85.Tp Cosmic-ray interactions

\*email: rprother@physics.adelaide.edu.au

# 1 Introduction

M87 is usually classified as a Fanaroff-Riley Class I (FR-I) radio galaxy having a one-sided relativistic jet [1] implying, in the context of unification models [2] that its unresolved nuclear region is a misaligned BL Lac object. The viewing angle is estimated to be  $\theta \approx 30^\circ$  giving a maximum Doppler factor  $\delta = [\gamma_j(1 - \beta_j \cos \theta)]^{-1}$  of  $\delta_{\max} \approx 2$  where  $\gamma_j = (1 - \beta_j^2)^{-1/2}$  is the jet Lorentz factor. For simplicity, we shall take  $\delta = 1$  but consider the range  $0.66 \leq \delta \leq 1.6$  for the M87 jet at pc scales. Although the jet emission is not strongly Doppler boosted towards us – it may even be de-boosted – its proximity to us (16.3 Mpc [3]) partially compensates for this, and makes TeV gamma-ray [4], cosmic ray [5, 6] and possibly neutrino emission from this object potentially interesting.

The strong variability of the optical flux of M87 suggests that the jet emits synchrotron radiation at optical frequencies somewhere within an unresolved central region less than 5 pc in diameter [7]. The jet has well-defined relativistic features, and it is remarkable that despite its low power the jet extends beyond 30 arcsec from the core [8], possibly being a remnant from when M87 was much more active. Given the large black hole mass  $3 \times 10^9 M_\odot$ , and the low jet luminosity  $5 \times 10^{44}$  erg s $^{-1}$  [9], the accretion disk must be currently in a low radiative state and provide little power to the jet. As a consequence, the heating of any torus is currently inefficient and would produce little attenuation of TeV gamma-ray signals although this would change if M87 returned to an active state commensurate with its high black hole mass [10].

BL Lac objects, along with flat-spectrum radio quasars are collectively referred to as blazars. BL Lacs may be high-frequency or low-frequency peaked (HBLs and LBLs). Their broad-band spectra consist of two spectral components which appear as broad ‘humps’ in the spectral energy distribution (SED), and are due to emission from a jet oriented at small angle with respect to the line-of-sight. The low-energy component, is generally believed to be synchrotron emission from relativistic electrons, and extends from the radio to UV or X-ray frequencies. The origin of the high-energy component, starting at X-ray or  $\gamma$ -ray energies and extending in some cases to TeV-energies, is uncertain.

For BL Lacs which have rather weak thermal emission, the favoured “leptonic model” is the so-called synchrotron-self Compton (SSC) model in which the same relativistic electrons responsible for the low energy synchrotron hump in the SED up-scatter synchrotron photons to high energies via the Inverse Compton effect. “Hadronic models” were proposed more than 10 years ago to explain the  $\gamma$ -ray emission from blazars [11]. Recently Mücke & Protheroe [12, 13] have discussed in detail the various contributing emission processes in the synchrotron proton blazar (SPB) model. In hadronic models the relativistic jet consists of relativistic proton and electron components, which again move relativistically along the jet. High-energy radiation is produced through photomeson production, and through proton and muon synchrotron radiation, and subsequent synchrotron-pair cascading in the highly magnetized environment. In the case of BL Lacs internal photon fields (i.e. produced by synchrotron radiation from the co-accelerated electrons) serve as the target for pion photoproduction. These models can, in principle, be distinguished from

leptonic models by the observation of high energy neutrinos generated in decay chains of mesons created in the photoproduction interactions (for a recent review see [14]).

In hadronic models, AGN would contribute also to the pool of extragalactic ultra-high energy cosmic rays (UHECR) through the decay outside the host galaxy of neutrons produced by photoproduction interactions (see [15] in the context of accretion shocks, and [16] in the context of jets) or by escape of protons directly accelerated at termination shocks of jets in giant radio lobes of Fanaroff-Riley Class II (FR-II) radio galaxies [17].

Greisen [18], and Zatsepin and Kuz'min [19] (GZK) showed that the nucleonic component of UHECR above  $10^{20}$  eV will be severely attenuated in the cosmic microwave background radiation (CMBR), primarily due to pion photoproduction interactions. At  $3 \times 10^{20}$  eV the mean free path is  $\sim 5$  Mpc and the energy-loss distance is  $\sim 20$  Mpc [20] (see Stanev et al. [21] for recent calculations). Thus, if the UHECR are extragalactic, one would expect their spectrum to cut off at  $\sim 10^{20}$  eV, the “GZK cut-off”. UHECR may have been observed with energies well above  $10^{20}$  eV (see Nagano and Watson [22] for a review including a discussion of models for the origin of the UHECR). However, very recent data from the two largest aperture high energy cosmic ray detectors are contradictory: AGASA [23] observes no GZK cut-off while HiRes [24] observes a cut-off consistent with the expected GZK cut-off. A systematic over-estimation of energy of about 25% by AGASA or under-estimation of energy of about 25% by HiRes could account the discrepancy [24], and the continuation of the UHECR spectrum to energies well above  $10^{20}$  eV is now far from certain. Nevertheless, if the spectrum does extend well beyond  $10^{20}$  eV, even though it is only an FR-I radio galaxy M87 is an attractive possibility for the origin of the UHECR [5, 6] because of its proximity.

## 2 SPB modelling M87 as a mis-aligned BL Lac

Mücke et al. [25] identified the critical parameters determining the properties of BL Lacs in the context of the SPB model and constructed the “average” synchrotron spectrum for each class, HBLs and LBLs, which served as the target photon distribution for their hadronic cascade. An extensive collection of blazar SEDs published by Ghisellini et al. [26] were used to construct the “average” SED of HBLs and LBLs by overlaying all available HBL and LBL SEDs. They found that a broken power law gave a reasonable representation of the low-frequency hump in the SED of both HBLs and LBLs

$$n(\epsilon) \propto \begin{cases} \epsilon^{-\alpha_1} & \text{for } \epsilon_i \leq \epsilon \leq \epsilon_b \\ \epsilon^{-\alpha_2} & \text{for } \epsilon_b \leq \epsilon \leq \epsilon_c \end{cases} \quad (1)$$

with  $\alpha_1 = 1.5$ ,  $\alpha_2 = 2.25$  and  $\epsilon_i = 10^{-5\ldots-6}$  eV. The break energy  $\epsilon_b$  of LBLs varied between  $\approx 0.1$  eV to 1.3 eV, while the maximum synchrotron photon energy  $\epsilon_c$  ranged over two orders of magnitude, from  $\approx 41$  eV to 4 keV. The populated energy range of HBLs is more restricted:  $\epsilon_b \approx 26$  eV to 131 eV and  $\epsilon_c \approx 4.1$  keV to 41 keV. The peak of the low-energy SED was  $\log \nu L_\nu^{\max}(\text{erg/s}) \approx 45.6 - 46.1$  for LBLs and  $\log \nu L_\nu^{\max}(\text{erg/s}) \approx 43.4 - 43.8$

for HBLs. Mücke et al. [25] defined the “average LBL” by  $\epsilon_b = 1.3$  eV,  $\epsilon_c = 4.1$  keV and  $\log \nu L_\nu^{\max}$  (erg/s) = 46.1, and the “average HBL” by  $\epsilon_b = 131$  eV,  $\epsilon_c = 41$  keV and  $\log \nu L_\nu^{\max} = 43.8$ . The parametrizations for HBLs and LBLs are visualized in Fig. 1, with the dashed lines showing the “average” SED and the hatched regions showing the range of the SEDs for the two cases.

Assuming that the unresolved nuclear emission in M87, i.e. from the pc scale jet, has  $\delta = 1$  we have added to Fig. 1 the radio [27], infrared [28] and X-ray [29] data on the nuclear region of M87 Doppler boosted by  $\delta = 10$  to mimic how M87 would appear if its jet were closely aligned towards us such that it would be classed as a BL Lac rather than a FR-I. Since the Doppler factor of M87 is not well known, taking the range from 0.66 to 1.5, the observed SED as viewed along the axis with  $\delta = 10$  would move along the error bars added to the data. From Fig. 1, the rather high radio-infrared luminosity would suggest that M87 could be a mis-aligned LBL, in which case the X-ray emission would be part of the high-energy hump in the SED due to cascading initiated by photons and electrons from pion decay or by synchrotron photons emitted by protons and muons. However, the X-ray emission is at a level closer to that expected from an HBL, in which case it would be mainly due to synchrotron emission by directly accelerated electrons. One should bear in mind that there is considerable variation in the SEDs of HBLs and LBLs, and so one should not expect the SED of an individual BL Lac to be identical to our “average” spectrum. This is particularly true for the M87 nuclear region where the observations at radio, infrared and X-rays were not simultaneous and are known to vary. In addition, Wilson and Yang [29] have calculated from the Chandra X-ray flux and spectrum observed from the inner part of the jet that there is intrinsic absorption by cold matter with an equivalent hydrogen column density of  $3\text{--}5 \times 10^{20}$  cm $^{-2}$  in M87, and so the unattenuated X-ray flux could be higher than plotted. Thus we shall be satisfied if the observed SED is within a factor  $\sim 2$  of an “average” SED.

In Fig. 2 we show the SEDs of HBLs modelled by Mücke et al. [25] in the context of the SPB model as they would appear if observed at  $\delta = 1$  as FR-I radio galaxies at a distance of 16 Mpc appropriate to M87. Results taken from Mücke et al. [25] for four peak luminosities of the low energy hump of the SED are shown after shifting to  $\delta = 1$ . As we see, there is little variation in the high energy hump which peaks at  $\sim 10\text{--}100$  GeV at a level just below the sensitivities of EGRET and the Whipple High Energy Gamma Ray Telescope, but well above the sensitivity of GLAST and future northern hemisphere large-area atmospheric Cherenkov telescopes (ACT) such as MAGIC and VERITAS (sensitivities for all these telescopes taken from ref. [30] are shown together with the upper limit from Whipple [31]). One should bear in mind, however, that the uncertainty in the Doppler factor of M87 will give rise to a much larger uncertainty in the bolometric luminosity. These uncertainties are indicated in the theoretical SED and neutrino spectra by the slanted error-bars. We have extended the work of Mücke et al. [25] by calculating the neutrino output for these four cases and plot the expected flux of muon-neutrinos ( $\nu_\mu + \bar{\nu}_\mu$ ). The highest luminosity modelled for the low-energy hump of the SED (solid curve) is in closest agreement with the M87 SED and predicts the highest

neutrino flux. We have added an upper-limit for the AMANDA-B10 neutrino telescope by taking the diffuse neutrino background limit [32] and multiplying by  $2\pi$  sr (neutrino telescopes detect upward-going neutrinos). Sensitivities calculated by Albuquerque et al. [33] of AMANDA-II and IceCube to  $E^{-2}$  diffuse intensity, again multiplied by  $2\pi$  sr to convert to point source sensitivity have also been added. Unlike the 100 GeV gamma-ray emission which should easily be detected by future telescopes, the neutrino flux is well below detection levels of future neutrino telescopes.

In Fig. 3 we model M87 as a mis-aligned LBL in the context of the SPB model. In this case, we see that the gamma-ray emission cuts off at 10 GeV–1 TeV depending on the luminosity of the low energy hump of the SED. This is because for the higher target photon densities in LBL, pion photoproduction losses determine the maximum proton energy, and hence the maximum gamma-ray energy which results from the cascades initiated by proton synchrotron radiation and pion decay (including pion and muon synchrotron radiation). This also affects the maximum neutrino energy in the same way. The lowest luminosity modelled for the low-energy hump of the SED (chain curve) is in closest agreement with the M87 SED and predicts the highest gamma-ray and neutrino energies. The gamma ray flux is a factor  $\sim 3$ –10 lower than for the HBL case, but is still detectable by future telescopes. As with the HBL case, the neutrino flux is below the sensitivity of IceCube. However, it is not impossible that in the case of rapid flaring, M87 might just be detected as it is at a declination of  $\sim +12^\circ$  and is ideally located for observation by a giant neutrino telescope to be located at the South Pole such as IceCube because it is sufficiently below the horizon to eliminate cosmic ray events, while not being so far below the horizon that neutrino absorption by the Earth’s core becomes important.

### 3 M87 as a source of UHECR

Energetic protons magnetically trapped in AGN jets lose energy predominantly by Bethe-Heitler pair production and pion photoproduction on ambient radiation fields, or by adiabatic deceleration as the jet expands. Neutron production in pion photoproduction sources (e.g.  $p\gamma \rightarrow n\pi^+$ ) provides a mechanism for escape of cosmic rays from the jet. Neutrons decay typically after travelling  $(E_n/10^{20}\text{eV})$  Mpc, which for UHECR is well outside the host galaxy. Recently Ahn et al. [5] and Biermann et al. [6] have shown that in the assumption of a Parker-spiral galactic wind magnetic structure out to  $\sim 1.5$  Mpc, the galactic wind of our Galaxy poses no restriction to the entry to our Galaxy of UHECR from the general direction of M87, and may even lead to clustering in the arrival directions of cosmic rays from M87 observed from Earth. These preferred arrival directions and clustering may, however, be mainly due to the Galactic wind topology and contain little information about the direction of cosmic ray sources [34].

The observed intensity of UHECR [35] (multiplied by energy squared) is plotted in Fig. 4. For the most promising LBL model (chain curve in Fig. 3) we plot (chain curve) the flux of neutrons divided by  $4\pi$  sr (to convert flux to average intensity) that would be observed at Earth from M87 if the neutrons did not decay (which of course they do).

Since these neutrons would travel to Earth in straight lines, and since we take M87 to have  $\delta(\theta \sim 30^\circ) = 1$ , the maximum neutron energy that would arrive at Earth would be approximately the maximum jet-frame energy of the accelerated protons, which would be  $E_n = 3 \times 10^{19}$  eV for the model shown. However, neutrons decay into protons whose directions are isotropised in the intergalactic magnetic field before and during propagation to Earth. Hence we would have contributions to the protons arriving at Earth from neutrons emitted at all angles with respect to the jet axis, and hence from the full range of Doppler factors corresponding to the jet Lorentz factor, i.e. approximately  $1/2\gamma_j \rightarrow 2\gamma_j$ . For example, if the jet Lorentz factor were  $\gamma_j = 5$  a neutron with jet-frame energy  $E'_n = 3 \times 10^{19}$  eV emitted along the jet axis ( $\theta = 0^\circ$ ) would decay to a proton with galaxy-frame energy  $E \approx 3 \times 10^{20}$  eV. What we would observe therefore depends on the galaxy-frame angle-averaged neutron luminosity *on emission*, and would also have contributions from both jets (i.e. twice that for one jet). Given that the chain curve in Fig. 4 is for  $\delta(\theta \sim 30^\circ) = 1$ , it is related directly to the jet-frame bolometric luminosity  $E'_n{}^2 \dot{N}'_n(E'_n)$ . For electromagnetic radiation and neutrinos the *observed* bolometric luminosity is  $\nu L_\nu^{\text{obs}}(\theta) = \delta^4(\theta) \nu' L'_\nu$ , and the angle-averaged *emitted* bolometric luminosity is  $\nu L_\nu^{\text{em}} = (4\pi)^{-1} \oint \delta^3(\theta) \gamma_j^{-1} \nu' L'_\nu d\Omega$ . Hence, by analogy, for ultra-relativistic protons of energy  $E \approx E_n$  from neutron decay, and remembering that both jets contribute,

$$E^2 \dot{N}(E) = \frac{2}{4\pi} \oint \delta^3(\theta) \gamma_j^{-1} E'_n{}^2 \dot{N}'_n(E'_n) d\Omega. \quad (2)$$

We have added to Fig. 4 (solid curve) the resulting cosmic ray flux divided by  $4\pi$  sr assuming  $\gamma_j = 5$  and straight-line propagation, i.e.

$$E^2 I(E) = \frac{E^2 \dot{N}(E)}{(4\pi) 4\pi d^2} \quad (3)$$

corresponding to number density

$$n(E) = \frac{\dot{N}(E)}{4\pi d^2 c}. \quad (4)$$

At  $5 \times 10^{19}$ – $3 \times 10^{20}$  eV this is a factor  $\sim 20$  below the observed UHECR.

Of course, so far this neglects effects of diffusive propagation to Earth and interactions with the CMBR. We shall consider first the effects of diffusion. For the case of a constant injection rate of cosmic rays, and an infinite homogeneous diffusing medium with diffusion coefficient  $D(E)$  the number density at distance  $d$  is simply

$$n(E) = \frac{\dot{N}(E)}{4\pi D(E) d}. \quad (5)$$

If we take  $D(E) = \lambda(E)c/3$  then the observed intensity will be enhanced with respect to straight-line propagation by a factor

$$g(E) = dc/D(E) = 3d/\lambda(E). \quad (6)$$

For a simple model of intergalactic space with a low magnetic field ( $\sim 10^{-9}$  G) and a cell size  $L_C > 100$  kpc, taking  $\lambda(E) \sim L_C$  would give an enhancement factor up to  $g(E) < 500$ , such that the predicted UHECR from M87 could explain the observed intensity above  $10^{19}$  eV. While diffusion appears to increase the cosmic ray intensity from M87, it also increases the travel time or effective distance travelled from M87 to Earth,

$$d_{\text{eff}} = d^2 c / 2D(E) = dg(E)/2. \quad (7)$$

Hence for an enhancement factor of  $g = 20$  the effective distance is  $d_{\text{eff}} = 160$  Mpc. At  $10^{19}$  eV the mean energy-loss distance is approximately 1 Gpc and at  $10^{20}$  eV the mean energy-loss distance is approximately 160 Mpc, and so in this case there would only be a significant energy loss above  $10^{20}$  eV.

The situation could actually be quite different if we consider an intergalactic magnetic field (IGMF) structure based on the observation of microgauss fields in clusters of galaxies [36], and of clusters occurring in networks of “walls” separated by “voids”. It would then be reasonable to expect relatively high fields of  $10^{-7}$ – $10^{-6}$  G in the walls, and much lower fields,  $10^{-11}$ – $10^{-9}$  G, in the voids. Recently, Stanev et al. [37] have considered propagation of UHECR in three different models of the IGMF in the local supergalactic structure in which the regular field in the high-field region was  $10^{-8}$  G. We consider propagation in a simple wall/void model similar to that used by Medina Tanco [38] to illustrate how UHECR would be deflected in complex IGMF structures. As M87 is at the centre of the Virgo Cluster and is close to the super-galactic plane we assume it is embedded in the higher field region. To illustrate the effect of propagation from M87 in a wall/void type IGMF we define the origin of coordinates to be at M87 with the mid-plane of the wall corresponding to the  $x$ – $y$  plane, the wall occupying  $|z| < 2.5$  Mpc and the void occupying  $|z| > 7.5$  Mpc. Following Medina Tanco [38] we adopt a regular magnetic field of  $10^{-7}$  G in the  $x$ -direction in the wall and  $10^{-10}$  G in the void, with a transition region sandwiched between the wall and the void in which the magnetic field drops exponentially from  $10^{-7}$  G to  $10^{-10}$  G. The magnetic field contains an irregular component having  $\langle |\vec{B}_{\text{irreg}}|^2 \rangle^{1/2}$  equal to 30% of the regular component, and has a Kolmogorov spectrum of turbulence. The irregular field is modelled as described in ref. [21] with wavenumbers corresponding to turbulence scales  $L_C/2^n$  with  $L_C = 2.5$  Mpc and  $n = 0, \dots, 3$ . Particles are injected isotropically at the origin and energy losses due to Bethe-Heitler pair production and pion photoproduction are included. A typical simulation for  $E_0 = 10^{20}$  eV is shown in Fig. 5.

Whereas Medina Tanco [38] was most interested in the angular deflection of arriving cosmic rays relative to the direction of the cosmic ray source, we are more interested in the travel times of cosmic rays to Earth from the distance  $d \approx 16$  Mpc to M87, and the total amount of time spent within unit volume at distance  $d$  from M87. We divide the spherical shell corresponding to  $15 \text{ Mpc} < d < 17 \text{ Mpc}$  into 2160 equal cells of volume  $V$  with a grid in spherical coordinates  $(\theta, \phi)$  using 72 equally spaced  $\phi$ -values and 30 equally spaced  $\cos \theta$ -values. Particle orbits are advanced in time steps of size  $\Delta t = 0.03$  Mpc/ $c$  chosen to be much smaller than the smallest magnetic structure simulated. At each step,

the proton energy is reduced according to the average energy-loss rate (see e.g. figure 1 of ref. [21]). A check is made at the end of each time step to determine whether the proton is within the spherical shell, and if it is then  $\Delta t$  is added to the total time spent in the cell corresponding to its spherical coordinates  $(\theta, \phi)$  – i.e. if on  $k$  occasions a particle was found to be located inside the  $i$ th cell at the end of a time step, then it would have spent approximately a total time  $k\Delta t$  inside the  $i$ th cell since being injected at the origin. Dividing by the number of simulations one obtains the average time spent in a particular cell per injected proton  $\tau(\theta, \phi)$ . Similarly, the time spent travelling since injection at M87 is added to the ages of the protons “detected” in that cell. Dividing by the total number of occasions a particle was “detected” in that cell gives the average age  $\bar{t}(\theta, \phi)$  of the protons present in that cell.

Results based on the average time per unit volume in  $10^6$  simulations are shown for two initial energies  $10^{19}$  eV and  $10^{20}$  eV in Fig. 6. The gray-scale shows the enhancement factor

$$g(\theta, \phi) = 4\pi d^2 c \tau(\theta, \phi) / V. \quad (8)$$

The strong peaks at  $(0^\circ, 0)$  and  $(180^\circ, 0)$  show that despite the presence of the turbulent field component, cross-field diffusion is not strong enough to give rise to significant fluxes far away from the regular field threading the source, at least for source distances as small as 16 Mpc for this field topology, and we note that Stanev et al. [37] arrived at a similar conclusion about cross-field diffusion. The peaks in  $g(\theta, \phi)$  shown in Fig. 6 are at a level  $g(\theta, \phi) \sim 10^3$  over a disk of radius  $\sim 5^\circ$  ( $\sim 1.4$  Mpc) outside of which  $g(\theta, \phi) \ll 1$ , indicating that if the magnetic field topology is such that the field lines connect the vicinity of M87 (within  $\sim 1$  Mpc) to our Galaxy (within  $\sim 1$  Mpc) then cosmic rays from M87 should clearly be observed. The average ages are  $\bar{t} \sim 200$  Mpc/c ( $E_0 = 10^{19}$  eV) and  $\bar{t} \sim 100$  Mpc/c ( $E_0 = 10^{20}$  eV) indicating their final energies would be  $\sim 8 \times 10^{18}$  eV and  $\sim 5 \times 10^{19}$  eV respectively.

## 4 Conclusion

We find the unresolved nuclear core of M87 to be consistent with it being a mis-aligned BL Lac object. In the context of the Synchrotron Proton Blazar model, M87 could be either an HBL or an LBL. In both cases, we predict gamma-ray emission at levels detectable by GLAST and MAGIC, and possibly by VERITAS. Neutrino detection is not expected, except possibly during an extreme flare in the LBL case.

Ultra-high energy neutrons produced in pion photoproduction interactions will escape from the host galaxy where they decay into protons. Because cosmic rays are deflected in the IGMF, protons resulting from neutrons emitted in all directions can contribute to the observed UHECR. Hence, even though the electromagnetic radiation we observe from the M87 jet is not significantly Doppler boosted in energy, the cosmic ray output will be. By this mechanism, the unresolved nuclear core of the M87 jet could emit UHECR with energies up to at least  $\sim 3 \times 10^{20}$  eV.

We predict the UHECR output from M87 to be at a level such that if UHECRs travelled in straight lines they would give an average intensity at Earth a factor  $\sim 20$  below that observed. For a constant UHECR output and simple isotropic diffusion with a scattering mean free path  $\lambda$  less than the distance  $d$  to M87, the predicted intensity would be enhanced by a factor  $3d/\lambda$  relative to straight line propagation. This enhancement is accompanied by increased travel times, and so higher energy losses in the CMBR. Nevertheless, taking reasonable scattering mean free paths we find that for simple diffusion models protons from decay of ultra-high energy neutrons produced by pion photoproduction in the M87 jet could easily account for all the observed UHECR.

In perhaps more realistic wall/void models of IGMF structure, M87 would only be a source of the observed UHECR if the topology of the IGMF between M87 and our Galaxy is favourable. Note, however, that because of its very high black hole mass M87 was probably much more active at earlier times than at present. Many objects exhibit a high state for  $\sim 5\%$  of the time, and since we estimate the average travel time of UHECR from M87 to Earth to be a factor  $\sim 5\text{--}10$  times the light propagation time it is indeed possible that the UHECR observed now were emitted when M87 was in a high state and possibly a more powerful cosmic ray source. Similarly, if M87 was in the recent past a powerful FR-II radio galaxy, it could have been possible to accelerate UHECR at shocks in the giant radio lobes where the jets terminate as in the model of Rachen and Biermann [17], and these could also contribute to the observed UHECR.

## Acknowledgments

We thank Todor Stanev for very helpful comments. This work was supported by a Discovery Project grant from the Australian Research Council and a grant from the University of Adelaide to RJP. AR thanks the Bundesministerium für Bildung und Forschung for financial support through DESY grant Verbundforschung 05CH1PCA/6.

## References

- [1] J. A. Biretta, in *The Radio Galaxy M87*, ed. H.-J. Röser & K. Meisenheimer (Springer: Berlin), (1999) 159.
- [2] C.M. Urry, P. Padovani, *PASP* 107 (1995) 803.
- [3] J.C. Cohen , *Astron. J.* 119 (2000) 162.
- [4] J. M. Bai, M. G. Lee, *Astrophys. J.* 549 (2001) L173
- [5] E.-J. Ahn, G. Medina-Tanco, P. L. Biermann, T. Stanev, [astro-ph/9911123](https://arxiv.org/abs/astro-ph/9911123)

- [6] P. L. Biermannn, E.-J. Ahn E.-J., , P. P. Kronberg, G. Medina-Tanco, T. Stanev, in Physics and Astrophysics of Ultra-High-Energy Cosmic Rays, Edited by M. Lemoine and G. Sigl, Lecture Notes in Physics, vol. 576, p. 181.
- [7] Z.I. Tsvetanov et al., *Astrophys. J.* 493 (1998) 83.
- [8] W. B. Sparks, J. A. Biretta, F. Macchetto, *Astrophys. J.* 473 (1996) 254.
- [9] F.N. Owen, J. A. Eilek, N. E. Kassim, *Astrophys. J.* 543 (2000) 611.
- [10] A.-C. Donea, R.J. Protheroe, in preparation
- [11] K. Mannheim, P.L. Biermann, *A&A* 221 (1989) 211.
- [12] Mücke A. & Protheroe R.J., *Proc. workshop "GeV-TeV Astrophysics: Toward a Major Atmospheric Cherenkov Telescope VI"*, AIP Conf. Proc. Vol 515, 149, eds.: B.D. Dingus et al. (2000)
- [13] A. Mücke, R.J. Protheroe, *Astropart. Phys.* 15 (2001) 121.
- [14] J. Learned, K. Mannheim, *Ann.Rev.Nucl.Part.Sci.* 50 (2000) 679.
- [15] R. J. Protheroe, A. P. Szabo, *Phys. Rev. Lett.*, 69 (1992) 2885.
- [16] K. Mannheim, R.J. Protheroe, J.P. Rachen, *Phys. Rev. D* 63 (2001) 023003.
- [17] J.P. Rachen, P.L. Biermann *A&A* 272 (1993) 161.
- [18] K. Greisen, *Phys. Rev. Lett.* 16 (1966) 748
- [19] G.T. Zatsepin, V.A. Kuz'min, *JETP Lett.* 4 (1966) 78.
- [20] F.W. Stecker, *Phys. Rev. Lett.* 21 (1968) 1016.
- [21] T. Stanev, R. Engel, A. Mücke, R.J. Protheroe, J.P. Rachen, *Phys. Rev. D* 62 (2000) 093005.
- [22] M. Nagano, A.A. Watson, *Rev. Mod. Phys.* 72 (2000) 689.
- [23] M. Takeda et al., [astro-ph/0209422](http://arxiv.org/abs/astro-ph/0209422)
- [24] T. Abu-Zayyad et al., [astro-ph/0208301](http://arxiv.org/abs/astro-ph/0208301)
- [25] A. Mücke, R.J. Protheroe, R. Engel, J.P. Rachen, T. Stanev, *Astropart. Phys.*, in press, [astro-ph/0206164](http://arxiv.org/abs/astro-ph/0206164)
- [26] G. Ghisellini et al., *MNRAS* 301 (1998) 451.
- [27] J. A. Biretta, C. P. Stern, D. E. Harris, *Astron. J.* 101 (1991) 1632.

- [28] E. S. Perlman, W. B. Sparks, J. Radomski, C. Packham, R. S. Fisher, R. Pina, J. A. Biretta, *Astrophys. J.* 561 (2001) L51
- [29] A.S. Wilson, Y. Yang, *Astrophys. J.* 568 (2002) 133 .
- [30] “GLAST: Exploring nature’s highest energy processes with the Gamma Ray Large Area Space Telescope” NASA document NP-2000-9-107-GSFC, February 2001, p29. <http://glast.gsfc.nasa.gov/resources/brochures/gsd/>
- [31] S. Lebohec and the VERITAS Collaboration, Proc. 27th Int. Cosmic Ray. Conf., Hamburg 2002, ed. M. Simon et al., Copernicus Gesellschaft, Katlenburg-Lindau, vol. 7, pp 2643-2645.
- [32] J. Ahrens, et al. (AMANDA Collaboration), in Proc. EPS International Conference on High Energy Physics, Budapest, 2001 (D. Horvath, P. Levai, A. Patkos, eds.), JHEP Proceedings Section, hep-ph/0112083
- [33] I.F.M. Albuquerque, J. Lamoureux, G.F. Smoot, hep-ph/0109177
- [34] P. Billoir, A. Letessier-Selvon, astro-ph/0001427
- [35] T.K. Gaisser, T. Stanev, in Particle Data Book, *Phys. Rev.* D66:010001 (2002) 182.
- [36] P. P. Kronberg, *Rep. Prog. Phys.* 57 (1994) 325
- [37] T. Stanev, D. Seckel, R. Engel, astro-ph/0108338
- [38] G.A. Medina Tanco, *Astrophys. J.* 505 (1998) L79

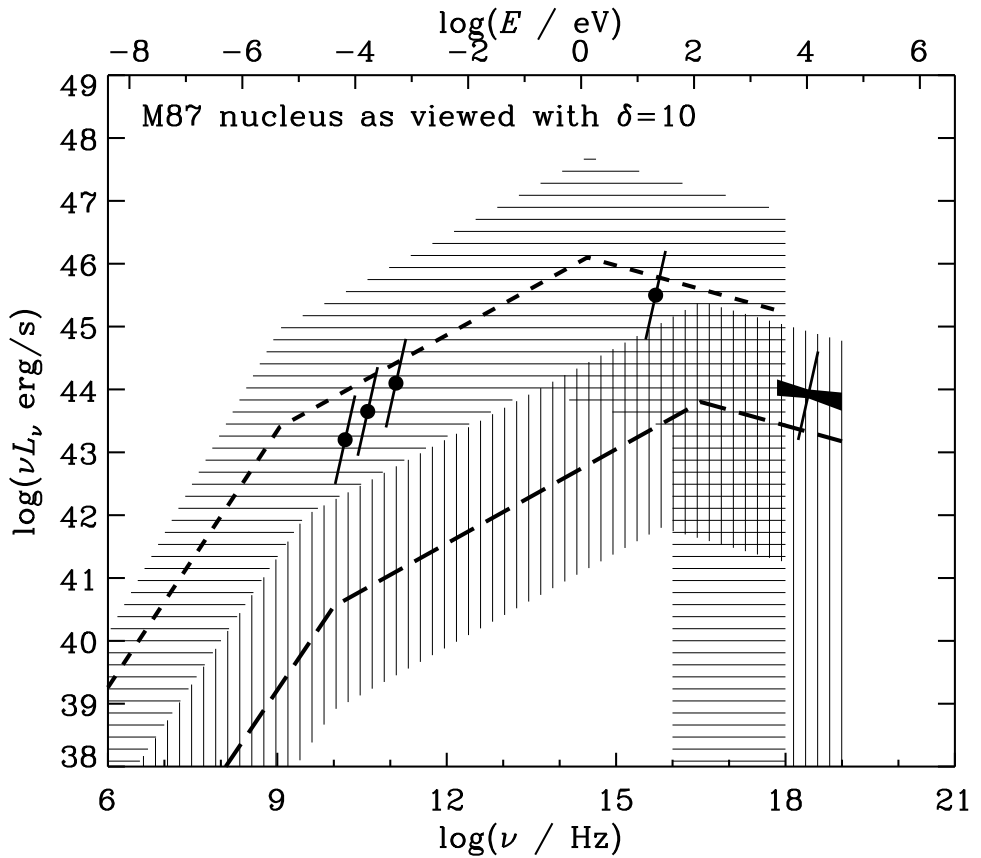


Figure 1: Form of the SED assumed for the synchrotron radiation from LBLs (short dashed curves) and HBLs (long dashed curves). The horizontal shading encompasses the SEDs of all LBLs, and the vertical shading encompasses the SEDs of all HBLs considered by Ghisellini et al. [26]. Data from M87 unresolved nuclear jet emission refs. [27, 28, 29] Doppler boosted to  $\delta = 10$  have been added (see text for details). Error bars correspond to uncertainty in Doppler boosting due to uncertainty in Doppler factor of M87 which we taken to be in the range  $0.67 \leq \delta \leq 1.5$ .

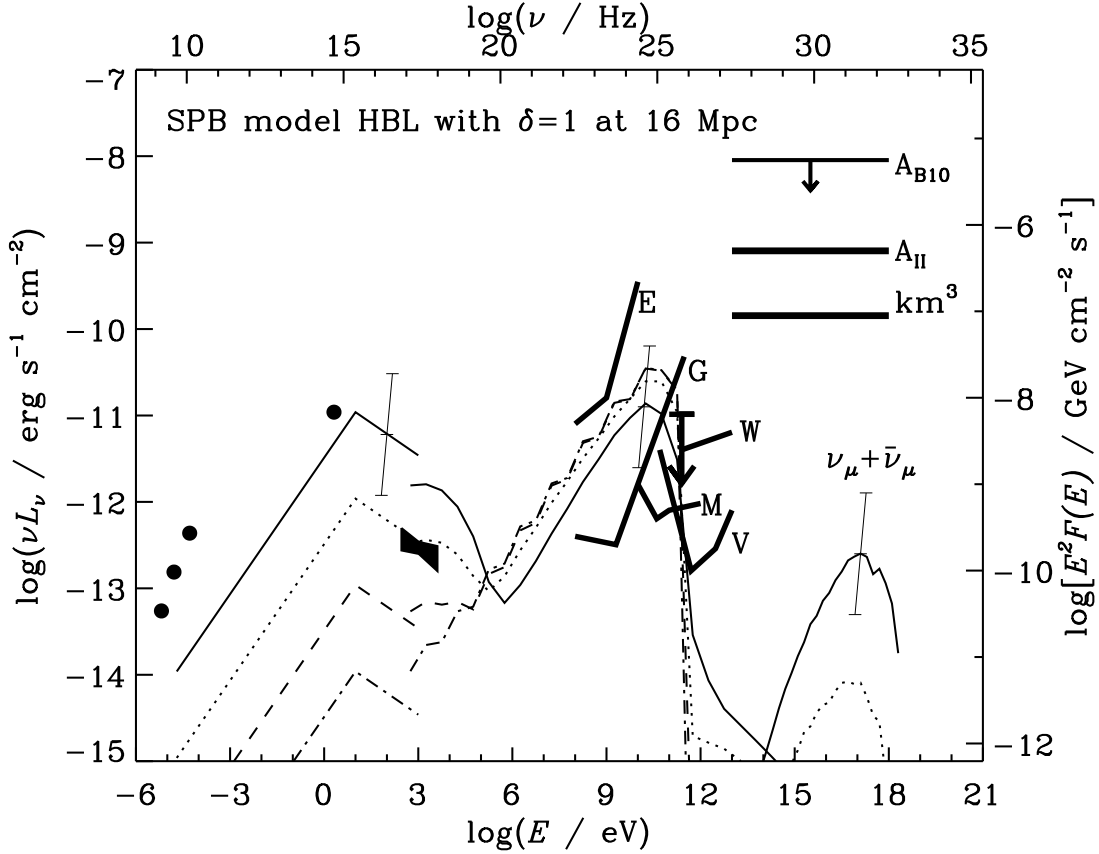


Figure 2: SED of emerging cascade radiation for different target photon spectra (broken power-laws shown),  $u'_B = u'_P$ ,  $B = 30G$ ,  $\delta = 1$ , and  $R' = 5 \times 10^{15}$  cm. HBL-like synchrotron spectra with  $u'_B = u'_P$ , and  $\log(u'_{\text{phot}}/\text{eVcm}^{-3}) = 8$  (chain curves), 9 (dashed curves), 10 (dotted curves) and 11 (solid curves). The broken power-laws on the left show the electron synchrotron radiation which provides the target photons for proton interactions, the curves in the range  $10^3$ – $10^{14}$  eV show the X-ray to gamma-ray flux due to proton interactions and proton synchrotron radiation and subsequent cascading, and the curves in the range  $10^{14}$ – $10^{18}$  eV show the corresponding neutrino fluxes (note that neutrino fluxes for  $\log(u'_{\text{phot}}/\text{eVcm}^{-3}) = 8$  and 9 are too low to be included in this plot). Error bars attached to solid curves correspond to uncertainty due to uncertainty in Doppler factor of M87 which we taken to be in the range  $0.67 \leq \delta \leq 1.5$ . The sensitivities of the EGRET (E), Whipple (W), GLAST (G), MAGIC (M) and VERITAS (V) gamma ray telescopes are indicated, as are the sensitivities of the AMANDA-II ( $A_{\text{II}}$ ) and IceCube ( $\text{km}^3$ ) neutrino telescopes, and an upper limit from AMANDA-B10 ( $A_{\text{B10}}$ ) – see text for details. Data from M87 unresolved nuclear jet emission refs. [27, 28, 29] and the upper limit at 250 GeV from Whipple [31] have been added.

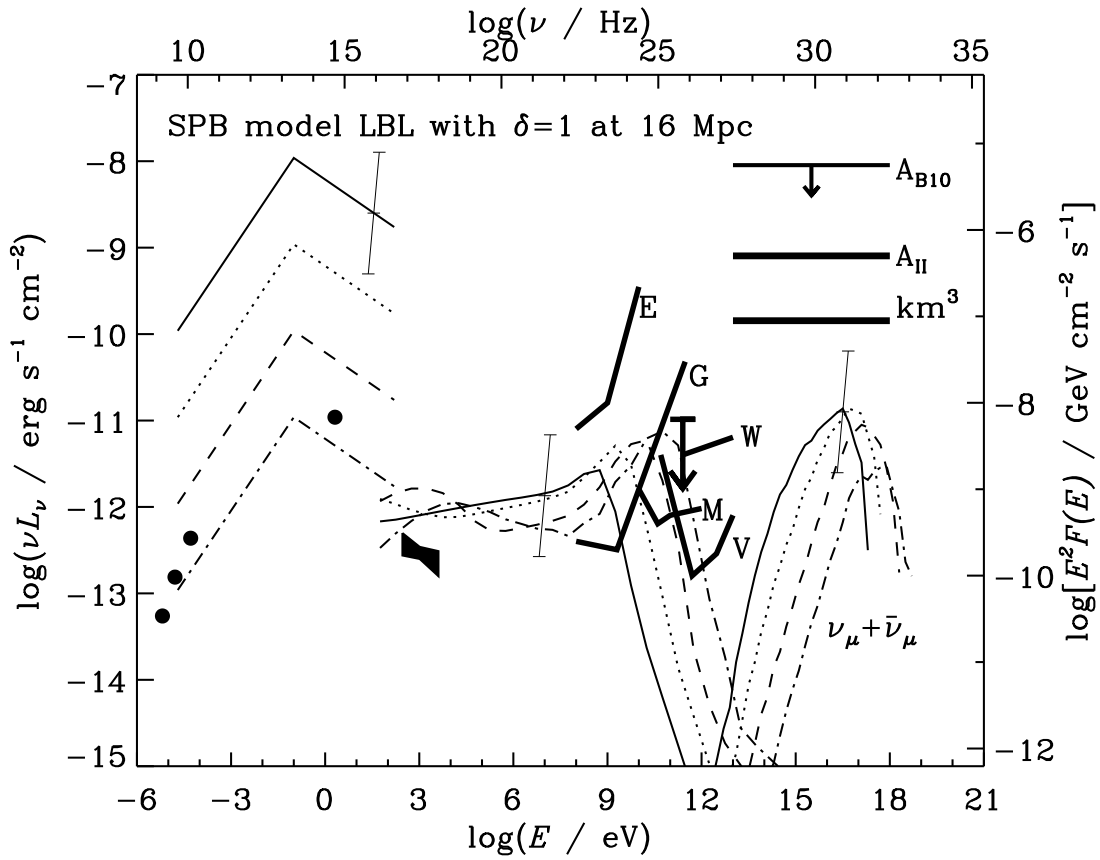


Figure 3: SED of emerging cascade radiation for different target photon spectra (broken power-laws shown),  $u'_B = u'_P$ ,  $B = 30G$ ,  $\delta = 1$ , and  $R' = 5 \times 10^{15} \text{ cm}$ . LBL-like synchrotron spectra with  $\log(u'_{\text{phot}}/\text{eVcm}^{-3}) = 11$  (chain curves), 12 (dashed curves), 13 (dotted curves) and 14 (solid curves). See Fig. 2 for key to other symbols.

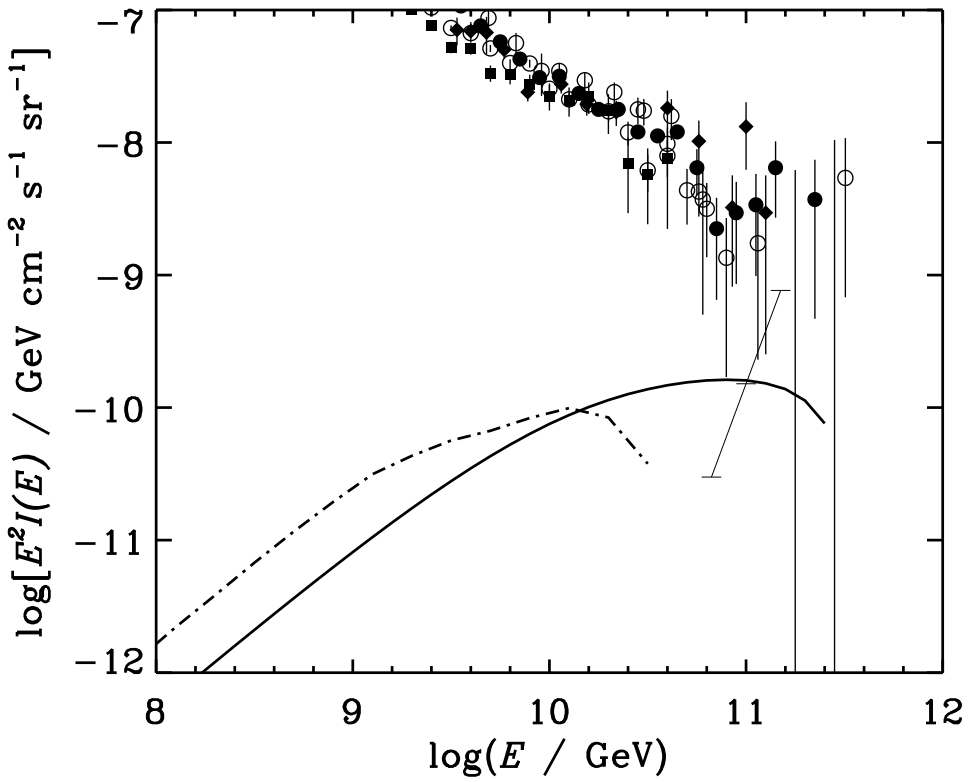


Figure 4: The observed intensity of UHECR taken from ref. [35]. Chain curve gives neutron flux divided by  $4\pi$  sr (to convert flux to average intensity) that would be observed at Earth from M87 if the neutrons did not decay (intensity shown corresponds to LBL model indicated by chain curve in Fig. 3). The solid curve is the cosmic ray intensity approximation given by Eq. 3 for this case (see text for a discussion of diffusion and energy-loss in the CMBR not included).

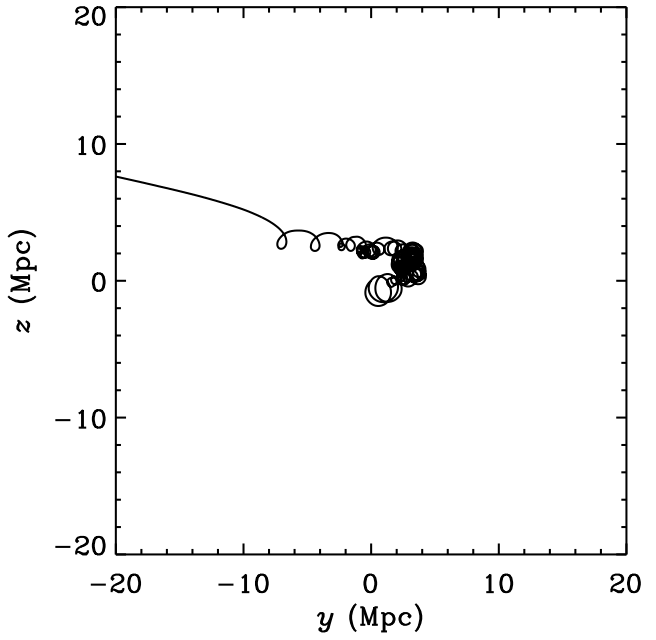
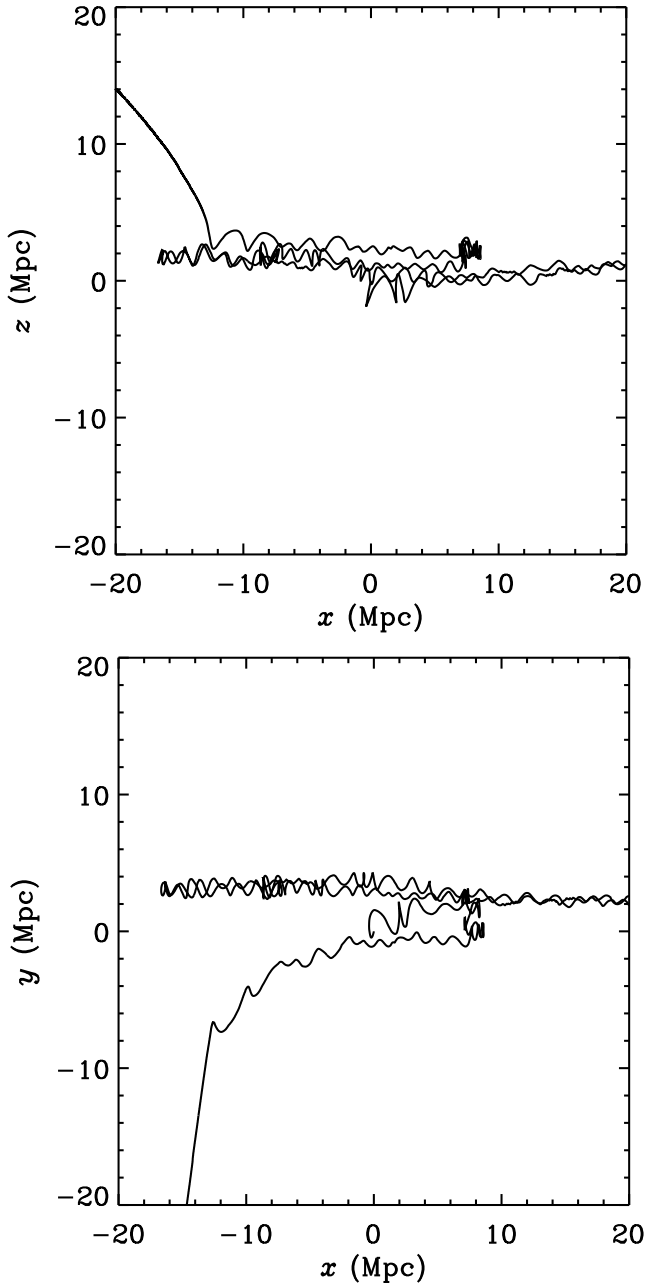


Figure 5: Three orthogonal views of a typical trajectory of a  $10^{20}$  eV proton in the wall/void model of the IGMF discussed in the text. Particle is injected at the origin, regular component of the magnetic field is in  $x$  direction. Wall extends from  $z = -2.5$  Mpc to  $z = 2.5$  Mpc.

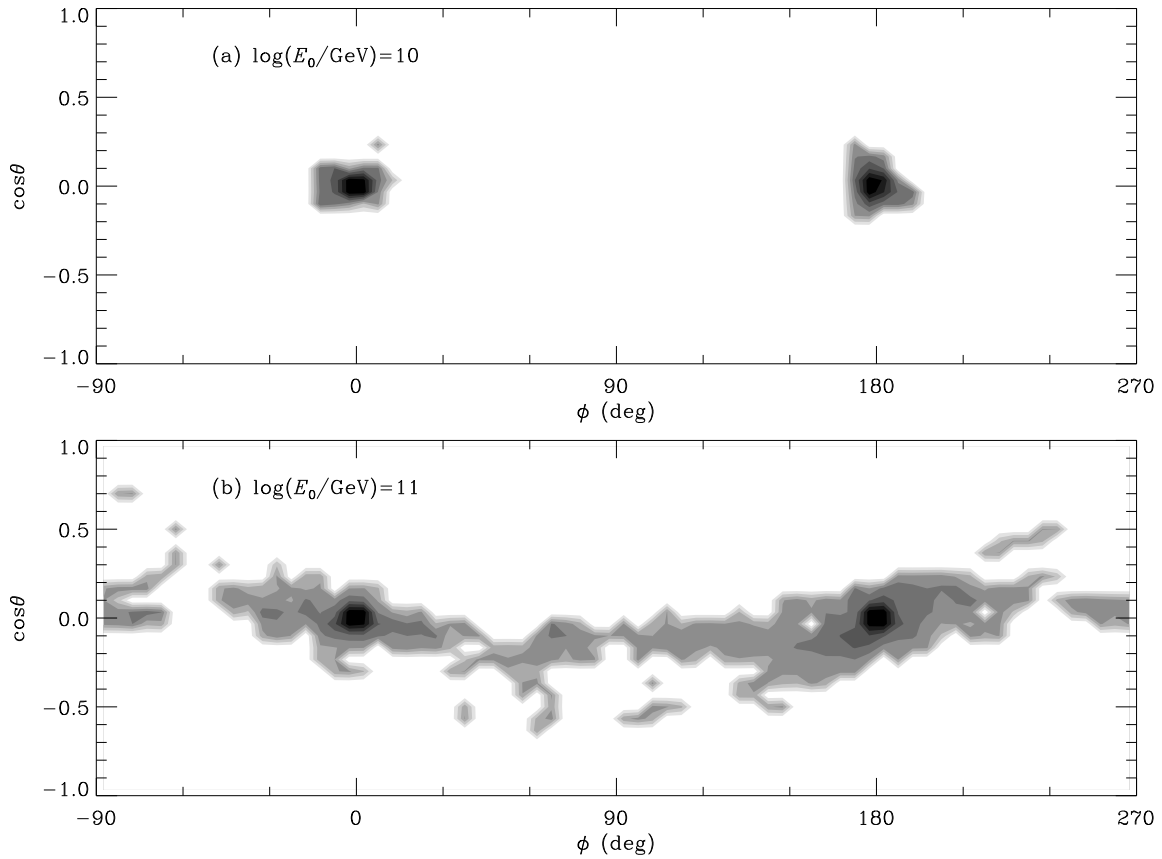


Figure 6: Enhancement factor  $g(E)$  (Eq. 8) as a function position  $(\theta, \phi)$  on a sphere of radius  $\sim 16$  Mpc centred on the origin for protons of initial energy (a)  $E_0 = 10^{19}$  eV and (b)  $E_0 = 10^{20}$  eV injected isotropically at the origin in the wall/void model of the IGMF discussed in the text. Gray-scale is logarithmic in  $g(E)$  (see text for details).